Received: Added at production | Revised: Added at production | Accepted: Added at production

DOI: xxx/xxxx

ARTICLE TYPE

Actuator and sensor fault estimation based on a proportional multiple-integral sliding mode observer for LPV systems with inexact scheduling parameters

S. Gómez-Peñate[1] | F.R. López-Estrada[1] | G. Valencia-Palomo[2] | D. Rotondo[3] | M.E. Guerrero-Sánchez[2,4]

[1]Tecnológico Nacional de México / IT Tuxtla Gutiérrez, TURIX-Dynamics - Diagnosis and Control Group, Chiapas, Mexico
[2]Tecnológico Nacional de México/ IT Hermosillo , Av. Tec. y Periférico Poniente SN, 83170, Sonora, Mexico
[3]Department of Electrical and Computer Engineering (IDE), University of Stavanger, Kristine Bonnevies vei 22, 4021 Stavanger, Norway
[4]Cátedras Conacyt

Correspondence
*Francisco-Ronay López-Estrada,
Email: frlopez@ittg.edu.mx

Summary

This paper proposes an approach for the estimation of states, actuator, and sensor faults in nonlinear systems represented by a polytopic linear parameter varying (LPV) system with inexact scheduling parameters. In the traditional LPV approaches, the scheduling variables are considered to be perfectly known. However, in practical applications, their measurement may contain precision and calibration errors or noise that can affect the performance of the diagnostic systems. Therefore, this work proposes the design of a proportional multiple-integral sliding mode observer (PMISMO) for fault diagnosis that copes with LPV systems with inexact scheduling parameters. Due to the introduction of some nonlinear functions, the proposed observer is a nonlinear parameter varying (NLPV) system for which stability and robustness performance are formulated using the Lyapunov technique and a H_∞ performance criterion. It is shown that the design conditions boil down to a set of linear matrix inequalities (LMIs) whose solution allows computing the observer gain matrix along with the tunable parameters of the nonlinear functions. Results obtained using the simulator of an octocopter-type unmanned aerial vehicle (UAV) are used to demonstrate the applicability and performance of the proposed fault diagnosis scheme.

KEYWORDS:
Nonlinear parameter varying (NLPV) systems, Fault diagnosis, Proportional multiple-integral sliding mode observer, Linear matrix inequalities (LMIs)

1 | INTRODUCTION

Modern control systems are prone to faults, which can damage the systems themselves or the environments in which they operate. For this reason, fault diagnosis (FD) algorithms become essential, since they enable fault-tolerant actions that minimize the effect of faults and improve the overall system's reliability and safety. An FD algorithm can be seen as a two-step process in which at first the fault is detected, i.e., a boolean logic value about the presence of a fault is provided, and then it is isolated, which means that its location is discovered. In many cases, fault estimation is also considered because it provides an information about the magnitude of the fault that can be sent to the fault-tolerant modules in order to improve the system's performance.[1]

Among the possible approaches to achieve fault detection, the model-based ones have been recognized as a handy tool by the scientific community and have been applied successfully to many physical systems, e.g. lateral dynamics of a vehicle[2], aerospace benchmarks,[3] aircraft,[4] satellites,[5] unmanned aerial vehicles,[6,7] and wind turbines,[8] among others. These approaches use a description of the process in terms of a mathematical model, so that the fault is detected by comparing discrepancies between the model and the estimated states.

Most physical systems are nonlinear, and therefore their fault diagnosis should employ nonlinear algorithms, which are difficult to generalize and apply in many cases. Convex mathematical models such as Takagi-Sugeno and quasi-linear parameter varying (quasi-LPV), have proved to be a good representation for systems with complex dynamics.[9,10] Convex systems are composed of a set of linear state-space models whose dynamics vary as a function of specific time-varying parameters. These functions are known as weighting functions, scheduling functions, or membership functions. It should not surprise that many works have proposed extensions of fault diagnosis approaches initially developed for LTI systems to convex systems.[11,12] In this way, the range of applicability of these approaches could be widened to include many nonlinear systems. For example, Rodriguez et al.[13] proposed an adaptable polytopic observer to estimate constant and time-varying actuator faults for LPV descriptor systems. Bedioui et al.[14] developed a robust adaptive observer to estimate sensor and actuator faults. Brizuela et al.[15] proposed to use an observer based on a polynomial LPV system for simultaneous actuator and sensor fault estimation. The solution presented in work by Li and Zhu[16] employed a reduced-order observer to accomplish this task. On the other hand, Li et al.[17] obtained the estimates using an unknown input proportional-integral observer.

The above works, similarly to the majority of the FD methods proposed for convex systems, assume that the scheduling variables can be measured correctly. However, in most cases, perfect knowledge of the scheduling variables is an unrealistic assumption, since in practice they are immeasurable or affected by strong uncertainties due to noise, offsets, low-quality, or uncalibrated sensors, among other factors.[18] If these limitations are not considered during the design, then the applicability and effectiveness of the FD methods are reduced, as discussed in the work by Zhang et al.[19]

Therefore, in a more realistic scenario, it is essential to take into account inexact scheduling variables in order to obtain an FD system that can be trustworthy and effective. This issue has been investigated by a few papers. For instance, the problem of robust fault detection observer design for convex systems with immeasurable scheduling variables was addressed by Aouaouda et al.[20] by means of a mixed H_-/H_∞ performance index. López-Estrada et al.[21] proposed a sensor fault estimation observer for descriptor LPV systems for which the influence of the error induced by the immeasurable scheduling variables was minimized using H_∞ optimization. Hassanabadi et al.[22] proposed a polytopic unknown input proportional-integral observer to estimate actuator faults in singular delayed LPV systems. Zhu and Zhao[23] dealt with switched LPV systems where they presented an approach for simultaneous control and fault detection in systems with inexact scheduling parameters. More recently, Gomez-Peñate et al.[24] proposed a method for simultaneous state and actuator/sensor fault estimation in quasi-LPV systems using a proportional-integral observer that took into account the uncertainty in the scheduling variables to enhance the performance and robustness. The original idea behind their work is that, apart from setting up a H_∞ optimization problem to constrain the effect that the exogenous disturbance and the faults have on the 2-norm of the output signal of interest, some nonlinear signals were introduced in the observer equations to compensate for the effect of the inexact scheduling variables. In this sense, their work fits into the innovative class of nonlinear parameter varying (NLPV) techniques[25,26] that, in contrast with traditional LPV techniques, maintain some nonlinear characteristics in the formulation, such as quadratic[27,28,29] and Lipschitz[30] terms.

It is well known that sliding mode techniques offer good potential for increasing the robustness of FD by including a nonlinear discontinuous term that depends on the output estimation error into the observer[31,32]. For this reason, there has been a lot of interest in using sliding mode observers for fault diagnosis,[33,34] with the development of extensions that allow for fault estimation in convex systems.[3,35] Notably, one of the recent research directions points towards obtaining design conditions for sliding mode FD schemes that can be applied to convex systems under the situation of imperfectly known scheduling parameters. For example, Chen et al.[36] have proposed an adaptive algorithm driven by an equivalent output error injection signal to adapt the values of the scheduling parameters used by the observer such that the performance level is maintained in spite of the mismatch between the real and the measured scheduling parameters.

In line with the recent developments, the main contribution of this work is to build upon the previous work reported in Gomez-Peñate et al.[24] by incorporating a sliding mode action which improves the performance of the fault estimation observer, in particular concerning the robustness to disturbances and uncertainty. Hence, this works presents the development of a proportional multiple-integral sliding mode observer (PMISMO) for LPV systems with inexact variables that achieves a simultaneous estimation of the system states and the time-varying actuator and sensor faults. Due to the introduction of some nonlinear functions, the proposed observer is an NLPV system for which stability and robustness requirements with respect to noise and

uncertainty in the scheduling variables are formulated in the form of linear matrix inequalities (LMIs).[37] The performance and effectiveness of the proposed observer are shown using results obtained with the simulator of an octorotor-type unmanned aerial vehicle (UAV).

The rest of the paper is organized as follows. Section 2 presents the background and problem description. Section 3 describes the design of the NLPV PMISMO for actuator and sensor fault estimation with inexact scheduling variables. Section 4 shows the simulation results obtained by applying the NLPV PMISMO to an octorotor UAV. Finally, Section 5 presents the conclusion and the proposed future work.

2 | PRELIMINARIES AND PROBLEM DESCRIPTION

Consider an LPV system affected by disturbances, sensor noise, as well as faults in sensors and actuators described by:

$$\begin{aligned}\dot{x}(t) =& A(\rho(t))x(t) + B(\rho(t))u(t) + F_a(\rho(t))f_a(t) + J(\rho(t))w(t),\\ y(t) =& C(\rho(t))x(t) + F_s(\rho(t))f_s(t) + D(\rho(t))w(t),\end{aligned} \tag{1}$$

where $x(t) \in \mathbb{R}^n$, $u(t) \in \mathbb{R}^{n_u}$, and $y(t) \in \mathbb{R}^{n_y}$, are the state, input and output vectors respectively. $f_a(t) \in \mathbb{R}^{n_{f_a}}$, $f_s(t) \in \mathbb{R}^{n_{f_s}}$ and $w(t) \in \mathbb{R}^{n_w}$ are actuator faults, sensor faults and exogenous disturbance/noise vectors respectively. $\rho(t) \in \mathbb{R}^q$ denotes the vector of scheduling parameters, for which dependence on time will be omitted from now on, in order to simplify the notation. $A(\rho) \in \mathbb{R}^{n\times n}$ denotes the state matrix, $B(\rho) \in \mathbb{R}^{n\times n_u}$ the input matrix, and $C(\rho) \in \mathbb{R}^{n_y\times n}$ the output matrix. $F_a(\rho) \in \mathbb{R}^{n\times n_{f_a}}$ and $F_s(\rho) \in \mathbb{R}^{n_y\times n_{f_s}}$ are the actuator and sensor fault distribution matrices, and $J(\rho) \in \mathbb{R}^{n\times n_w}$, $D(\rho) \in \mathbb{R}^{n_y\times n_w}$ are the disturbance/noise distribution matrices, respectively. It is assumed that $F_a(\rho)$ and $F_s(\rho)$ are full rank, and that there is no interdependence between different scheduling variables. Then, if the scheduling variables bounds are known, (1) can be represented by a polytopic LPV model with 2^q vertices with matrices $\mathcal{S} = \{A(\rho), B(\rho), C(\rho), D(\rho), J(\rho), F_a(\rho), F_s(\rho)\}$, such as:

$$\mathcal{S} = \left\{ \Upsilon(\rho) | \Upsilon(\rho) = \sum_{i=1}^{2^q} \alpha_i(\rho)\Upsilon_i; 0 \le \alpha_i(\rho) \le 1; \sum_{i=1}^{2^q} \alpha_i(\rho) = 1 \right\}, \tag{2}$$

where $\Upsilon_i = \{A_i, B_i, C_i, D_i, J_i, F_{a,i}, F_{s,i}\}$ and, for each vertex, the values of the matrix set is known. The weighting functions $\alpha_i(\rho)$ can be computed online since the values of the scheduling variables are measured in real-time.

It is important to note that if the scheduling variables were measured perfectly, the weighting factor could be used straightforwardly for the design of control systems elements such as controllers and observers. Nevertheless, in many cases, these parameters cannot be measured with high accuracy. For example, in electric vehicles, the speed is estimated through the rotation of the motors, the radius of the tires, the drive train, among other factors that change continuously with respect to time, and therefore the estimated speed is not exact. These differences between the measured and the real values affect the weighting factors and could deteriorate or destabilize the system. Therefore, the use of a robust approach that takes into account inexact scheduling parameters is required to ensure stability and performance requirements not only under sensor noise and disturbance but also under the inexact scheduling variables. To solve this problem, the weighting factors are assumed hereafter to be described by:

$$\alpha_i(\rho) = \lambda_i(t)\hat{\alpha}_i(\hat{\rho}), \tag{3}$$

where the terms $\hat{\alpha}_i(\hat{\rho})$ are uncertain due to the inexact scheduling variables denoted as $\hat{\rho}$; $\lambda_i(t)$ are the uncertainty factors, which are bounded by minimum and maximum values, denoted as $\underline{\lambda}_i$ and $\overline{\lambda}_i$, respectively. Then, the elements of (2) can be rewritten as:

$$\Upsilon(\rho) = \sum_{i=1}^{2^q} \alpha_i(\rho)\Upsilon_i = \sum_{i=1}^{2^q} \lambda_i(t)\hat{\alpha}_i(\hat{\rho})\Upsilon_i = \sum_{i=1}^{2^q} \hat{\alpha}_i(\hat{\rho})(\Upsilon_i + (\lambda_i(t) - 1)\Upsilon_i) = \sum_{i=1}^{2^q} \hat{\alpha}_i(\hat{\rho})\left(\Upsilon_i + \Delta\Upsilon_i(t)\right), \tag{4}$$

with $\sum_{i=1}^{2^q} \hat{\alpha}_i(\hat{\rho}) = 1$ and:

$$\Delta\Upsilon_i(t) = (\lambda_i(t) - 1)\Upsilon_i. \tag{5}$$

Based on the above discussion, (1) can be expressed as the following uncertain system:

$$\begin{aligned}\dot{x}(t) =& \left(A(\hat{\rho}) + \Delta A(\hat{\rho})\right)x(t) + \left(B(\hat{\rho}) + \Delta B(\hat{\rho})\right)u(t) + \left(F_a(\hat{\rho}) + \Delta F_a(\hat{\rho})\right)f_a(t) + \left(J(\hat{\rho}) + \Delta J(\hat{\rho})\right)w(t),\\ y(t) =& \left(C(\hat{\rho}) + \Delta C(\hat{\rho})\right)x(t) + \left(F_s(\hat{\rho}) + \Delta F_s(\hat{\rho})\right)f_s(t) + \left(D(\hat{\rho}) + \Delta D(\hat{\rho})\right)w(t).\end{aligned} \tag{6}$$

In order to estimate actuator and sensor faults simultaneously, the LPV system (6) is transformed by introducing $z(t) \in \mathbb{R}^{n_y}$, which is a filtered version of $y(t)$,[38,14] updated as $\dot{z}(t) = E\,(y(t) - z(t))$, where E is any Hurwitz matrix with appropriate dimensions, as shown in Figure 1.

By defining augmented state and fault vectors as $X(t) = \left[\, x(t)^T \;\; z(t)^T \,\right]^T \in \mathbb{R}^{\bar{n}}$ and $f(t) = \left[\, f_a(t)^T \;\; f_s(t)^T \,\right]^T \in \mathbb{R}^{n_f}$ with $\bar{n} = n + n_y$, $n_f = n_{f_a} + n_{f_s}$, the dynamics of the augmented system is expressed by:

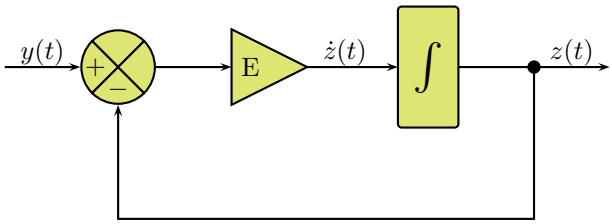

FIGURE 1 Block diagram of the filter.

$$\begin{aligned}\dot{X}(t) =& (\bar{A}(\hat{\rho}) + \Delta\bar{A}(\hat{\rho}))X(t) + (\bar{B}(\hat{\rho}) + \Delta\bar{B}(\hat{\rho}))u(t) + (\bar{F}(\hat{\rho}) + \Delta\bar{F}(\hat{\rho}))f(t) + (\bar{H}(\hat{\rho}) + \Delta\bar{H}(\hat{\rho}))w(t),\\ Y(t) =& z(t) = \bar{C}X(t),\end{aligned} \tag{7}$$

with:

$$\bar{A}(\hat{\rho}) = \begin{bmatrix} A(\hat{\rho}) & 0 \\ EC(\hat{\rho}) & -E \end{bmatrix}, \quad \Delta\bar{A}(\hat{\rho}) = \begin{bmatrix} \Delta A(\hat{\rho}) & 0 \\ E\Delta C(\hat{\rho}) & 0 \end{bmatrix}, \quad \bar{B}(\hat{\rho}) = \begin{bmatrix} B(\hat{\rho}) \\ 0 \end{bmatrix}, \quad \Delta\bar{B}(\hat{\rho}) = \begin{bmatrix} \Delta B(\hat{\rho}) \\ 0 \end{bmatrix}, \quad \bar{C} = \begin{bmatrix} 0 & I_{n_y} \end{bmatrix}$$

$$\bar{F}(\hat{\rho}) = \begin{bmatrix} F_a(\hat{\rho}) & 0 \\ 0 & EF_s(\hat{\rho}) \end{bmatrix}, \; \Delta\bar{F}(\hat{\rho}) = \begin{bmatrix} \Delta F_a(\hat{\rho}) & 0 \\ 0 & E\Delta F_s(\hat{\rho}) \end{bmatrix}, \; \bar{H}(\hat{\rho}) = \begin{bmatrix} J(\hat{\rho}) \\ ED(\hat{\rho}) \end{bmatrix}, \; \Delta\bar{H}(\hat{\rho}) = \begin{bmatrix} \Delta J(\hat{\rho}) \\ E\Delta D(\hat{\rho}) \end{bmatrix}.$$

Note that in the augmented system (7), sensor and actuator faults are embedded in a single fault vector $f(t)$ and the matrix $\bar{F}(\hat{\alpha})$ is full column rank.

Assumption 1. The faults $f(t)$ are assumed to be time-varying signals whose $k-$th time derivatives are bounded by f_0:[38]

$$\begin{aligned}\dot{f}(t) &= f_1(t),\\ \dot{f}_1(t) &= f_2(t),\\ &\vdots\\ \dot{f}_{k-1}(t) &= f_k(t),\\ f_k(t) &\leq f_0.\end{aligned} \tag{8}$$

The following Lemma will be consider to derived our main result:

Lemma 1. (Ichalal et al.[39]) Given matrices X and Y of suitable dimensions, the following property holds for any $\mu > 0$:

$$X^TY + Y^TX \leq \mu X^TX + \mu^{-1}Y^TY.$$

3 | PROPORTIONAL MULTIPLE-INTEGRAL SLIDING MODE OBSERVER

The proposed NLPV PMISMO estimates system states and faults simultaneously regardless of inexact scheduling variables, and is defined as follows:

$$
\begin{aligned}
\dot{\hat{X}}(t) =& \bar{A}(\hat{\rho})\hat{X}(t) + \bar{B}(\hat{\rho})u(t) + \bar{F}(\hat{\rho})\hat{f}(t) + K_P(\hat{\rho})sign\left(S(t)\right) + \varphi_x(\hat{\rho}),\\
\dot{\hat{f}}(t) =& K_I(\hat{\rho})\left(Y(t) - \hat{Y}(t)\right) + \hat{f}_1(t) + \varphi_f(\hat{\rho}),\\
\dot{\hat{f}}_1(t) =& K_{I_1}(\hat{\rho})\left(Y(t) - \hat{Y}(t)\right) + \hat{f}_2(t) + \varphi_{f_1}(\hat{\rho}),\\
&\vdots\\
\dot{\hat{f}}_{k-2}(t) =& K_{I_{k-2}}(\hat{\rho})\left(Y(t) - \hat{Y}(t)\right) + \hat{f}_{k-1}(t) + \varphi_{f_{k-2}}(\hat{\rho}),\\
\dot{\hat{f}}_{k-1}(t) =& K_{I_{k-1}}(\hat{\rho})\left(Y(t) - \hat{Y}(t)\right) + \varphi_{f_{k-1}}(\hat{\rho}),\\
\hat{Y}(t) =& \bar{C}\hat{X}(t),
\end{aligned}
\tag{9}
$$

where $K_P(\hat{\rho})$ and $K_I(\hat{\rho})$, $K_{I_1}(\hat{\rho})$, …, $K_{I_{k-1}}(\hat{\rho})$ denote the proportional and integral gains, respectively, that must be designed; $\varphi_x(\hat{\rho})$, and $\varphi_f(\hat{\rho})$, $\varphi_{f_1}(\hat{\rho})$, …, $\varphi_{f_{k-1}}(\hat{\rho})$ are signals that compensate for the effects of the inexact scheduling variables, as shown later in Theorem 1. $S(t) \in \mathbb{R}^{n_y}$ is the sliding surface, defined as $S(t) = Y(t) - \hat{Y}(t)$. In order to determine the gain $K_P(\hat{\rho})$, the following representation of $sign(S(t))$ is used:[40]

$$
sign(S(t)) = S(t) \oslash |S(t)| = S(t) - S(t) \circ \left(|S(t)| - 1_{n_y}\right) \oslash |S(t)| \tag{10}
$$

where $|S(t)|$ denotes the elementwise absolute value of $S(t)$, 1_{n_y} is the column vector of 1s with length n_y, and the symbols $\circ$ and $\oslash$ denote the Hadamard product and division, respectively.

Considering (8), the augmented form of the LPV model (7) and the NLPV PMISMO (9) are given by:

$$
\begin{aligned}
\dot{\bar{X}}(t) =& (\mathcal{A}(\hat{\rho}) + \Delta\mathcal{A}(\hat{\rho}))\bar{X}(t) + (\mathcal{B}(\hat{\rho}) + \Delta\mathcal{B}(\hat{\rho}))u(t) + (G(\hat{\rho}) + \Delta G(\hat{\rho}))w(t) + Rf_k(t),\\
\bar{Y}(t) =& C\bar{X}(t),
\end{aligned}
\tag{11}
$$

and:

$$
\begin{aligned}
\dot{\hat{\bar{X}}}(t) =& \mathcal{A}(\hat{\rho})\hat{\bar{X}}(t) + \mathcal{B}(\hat{\rho})u(t) + \mathcal{K}(\hat{\rho})(\bar{Y}(t) - \hat{\bar{Y}}(t)) - K_s(\hat{\rho}) + \varphi(\hat{\rho}),\\
\hat{\bar{Y}}(t) =& C\hat{\bar{X}}(t),
\end{aligned}
\tag{12}
$$

respectively, where:

$$
\bar{X}(t) = \begin{bmatrix} X(t) \\ f(t) \\ f_1(t) \\ \vdots \\ f_{k-1}(t) \end{bmatrix}, \quad \hat{\bar{X}}(t) = \begin{bmatrix} \hat{X}(t) \\ \hat{f}(t) \\ \hat{f}_1(t) \\ \vdots \\ \hat{f}_{k-1}(t) \end{bmatrix}, \quad \varphi(\hat{\rho}) = \begin{bmatrix} \varphi_x(\hat{\rho}) \\ \varphi_f(\hat{\rho}) \\ \varphi_{f_1}(\hat{\rho}) \\ \vdots \\ \varphi_{f_{k-1}}(\hat{\rho}) \end{bmatrix},
$$

with $\bar{X}(t) \in \mathbb{R}^{n_k}$, $\varphi(\hat{\rho}) \in \mathbb{R}^{n_k}$, $n_k = \bar{n} + k \times n_f$ and $\bar{e}(t) = \bar{X}(t) - \hat{\bar{X}}(t)$,

$$
\mathcal{A}(\hat{\rho}) = \begin{bmatrix} \bar{A}(\hat{\rho}) & \bar{F}(\hat{\rho}) & 0 & 0 & \dots & 0 \\ 0 & 0 & I_{n_k} & 0 & \dots & 0 \\ 0 & 0 & 0 & I_{n_k} & \dots & 0 \\ \vdots & \vdots & \vdots & \vdots & \vdots & \vdots \\ 0 & 0 & 0 & 0 & \dots & 0 \end{bmatrix}, \mathcal{B}(\hat{\rho}) = \begin{bmatrix} \bar{B}(\hat{\alpha}) \\ 0 \\ 0 \\ \vdots \\ 0 \end{bmatrix}, \mathcal{K}(\hat{\rho}) = \begin{bmatrix} K_P(\hat{\rho}) \\ K_I(\hat{\rho}) \\ K_{I_1}(\hat{\rho}) \\ \vdots \\ K_{I_{k-1}}(\hat{\rho}) \end{bmatrix}, \Delta\mathcal{B}(\hat{\rho}) = \begin{bmatrix} \Delta\bar{B}(\hat{\rho}) \\ 0 \\ 0 \\ \vdots \\ 0 \end{bmatrix}, R = \begin{bmatrix} 0 \\ 0 \\ 0 \\ \vdots \\ I_{n_f} \end{bmatrix}
$$

$$
\Delta\mathcal{A}(\hat{\rho}) = \begin{bmatrix} \Delta\bar{A}(\hat{\rho}) & \Delta\bar{F}(\hat{\rho}) & 0 & 0 & \dots & 0 \\ 0 & 0 & 0 & 0 & \dots & 0 \\ 0 & 0 & 0 & 0 & \dots & 0 \\ \vdots & \vdots & \vdots & \vdots & \vdots & \vdots \\ 0 & 0 & 0 & 0 & \dots & 0 \end{bmatrix}, G(\hat{\rho}) = \begin{bmatrix} \bar{H}(\hat{\rho}) \\ 0 \\ 0 \\ \vdots \\ 0 \end{bmatrix}, \Delta G(\hat{\rho}) = \begin{bmatrix} \Delta\bar{H}(\hat{\rho}) \\ 0 \\ 0 \\ \vdots \\ 0 \end{bmatrix}, K_s(\hat{\rho}) = \begin{bmatrix} K_P(\hat{\rho})S_y(t) \\ 0 \\ 0 \\ \vdots \\ 0 \end{bmatrix},
$$

$$
C = \begin{bmatrix} \bar{C} & 0 & 0 & 0 & \dots & 0 \end{bmatrix}, S_y(t) = S(t) \circ \left(|S(t)| - 1_{n_y}\right) \oslash |S(t)|.
$$

$\Delta\mathcal{A}(\hat{\rho})$, $\Delta\mathcal{B}(\hat{\rho})$ and $\Delta G(\hat{\rho})$ are unknown and time-varying matrices with appropriate dimensions. These matrices represent the model uncertainties, which are due to the inaccurate measurement of the scheduling variables and are related to equation (5). For further reasoning, the following assumption is considered:

Assumption 2. The uncertainties are bounded by:

$$\|\Delta\mathcal{A}_i(t)\| \leq \zeta_{1,i}, \tag{13}$$

$$\|\Delta\mathcal{B}_i(t)\| \leq \zeta_{2,i}, \tag{14}$$

$$\|\Delta G_i(t)\| \leq \zeta_{3,i}, \tag{15}$$

with positives scalars $\zeta_{1,i}$, $\zeta_{2,i}$ and $\zeta_{3,i}$.

A consequence of Assumption 2 is that the following inequalities hold true:

$$||\Delta\mathcal{A}(\hat{\rho})|| = ||\sum_{i=1}^{2^q} \hat{\alpha}_i \Delta\mathcal{A}_i(t)|| \leq \sum_{i=1}^{2^q} \hat{\alpha}_i ||\Delta\mathcal{A}_i(t)|| \leq \sum_{i=1}^{2^q} \hat{\alpha}_i \zeta_{1,i} = \zeta_1(\hat{\rho}), \tag{16}$$

$$||\Delta\mathcal{B}(\hat{\rho})|| = ||\sum_{i=1}^{2^q} \hat{\alpha}_i \Delta\mathcal{B}_i(t)|| \leq \sum_{i=1}^{2^q} \hat{\alpha}_i ||\Delta\mathcal{B}_i(t)|| \leq \sum_{i=1}^{2^q} \hat{\alpha}_i \zeta_{2,i} = \zeta_2(\hat{\rho}), \tag{17}$$

$$||\Delta G(\hat{\rho})|| = ||\sum_{i=1}^{2^q} \hat{\alpha}_i \Delta G_i(t)|| \leq \sum_{i=1}^{2^q} \hat{\alpha}_i ||\Delta G_i(t)|| \leq \sum_{i=1}^{2^q} \hat{\alpha}_i \zeta_{3,i} = \zeta_3(\hat{\rho}), \tag{18}$$

where the explicit dependence of $\hat{\alpha}_i$ and $\hat{\rho}$ has been omitted to relieve the notation. The evolution of the augmented state estimation error, denoted as $\dot{\bar{e}}(t)$, is given by:

$$\dot{\bar{e}}(t) = \Big(\mathcal{A}(\hat{\rho}) - \mathcal{K}(\hat{\rho})\mathcal{C}\Big)\bar{e}(t) + \Delta\mathcal{A}(\hat{\rho})\bar{X}(t) + \Delta\mathcal{B}(\hat{\rho})u(t) + \Delta G(\hat{\rho})w(t) + W(\hat{\rho})v(t) + K_s(\hat{\rho}) - \varphi(\hat{\rho}), \tag{19}$$

where:

$$v(t) = \begin{bmatrix} f_k(t) \\ w(t) \end{bmatrix} \quad \text{and} \quad W(\hat{\rho}) = \begin{bmatrix} R & G(\hat{\rho}) \end{bmatrix}. \tag{20}$$

Equation (19) is associated with the state vector $\bar{X}(t)$, the input $u(t)$, the noise $w(t)$, and the function $\varphi(\hat{\rho})$. The design goal is to select a gain $\mathcal{K}(\hat{\rho})$ which makes (19) asymptotically stable, hence ensuring that the estimation error will converge to zero when there are no uncertainties. Let us define the new variable:

$$\xi(t) = L\bar{e}(t), \tag{21}$$

where L is a constant matrix that is chosen by the designer to express which elements of $\bar{e}(t)$ should be prioritized when rejecting the effect of $v(t)$ using the $\mathcal{H}_\infty$ performance index. The following theorem provides the conditions to tune the observer gain $\mathcal{K}(\hat{\rho})$ and the discontinuous function $\varphi(\hat{\rho})$, such that the system (19) is asymptotically stable (in the sense of the estimation error converging to zero when there are no uncertainty and noise), and the effect of $v(t)$ onto the signal $\xi(t)$ is bounded by:

$$\|\xi(t)\|_2 < \gamma\|v(t)\|_2, \tag{22}$$

where $\|\cdot\|_2$ denotes the 2-norm of a $\mathcal{L}_2$-bounded signal and γ is the $\mathcal{H}_\infty$ performance index.

It is important to emphasize that the $\mathcal{H}_\infty$ performance index γ quantifies the influence of the disturbance $v(t)$ over the signal $\xi(t)$. The goal is to make the value of the performance index γ as small as possible.

Theorem 1. Given a scalar $\gamma > 0$, let $P > 0$, matrices M_i and positive scalars μ_2, μ_5, μ_6, μ_8 be such that the following set of LMI is feasible:

$$\begin{bmatrix} \Lambda_i + L^T L & PR & PG_i & P & \zeta_{1,i}I & \zeta_{2,i}P & \zeta_{3,i}P \\ * & -\gamma^2 I & 0 & 0 & 0 & 0 & 0 \\ * & * & (\mu_6 - \gamma^2)I & 0 & 0 & 0 & 0 \\ * & * & * & -\mu_8 I & 0 & 0 & 0 \\ * & * & * & * & -\mu_2 I & 0 & 0 \\ * & * & * & * & * & -\mu_5 I & 0 \\ * & * & * & * & * & 0 & -\mu_6 I \end{bmatrix} < 0, \qquad i = 1, \ldots, 2^q \tag{23}$$

with:

$$\Lambda_i = \mathcal{A}_i^T P + P\mathcal{A}_i - C^T M_i^T - M_i C,$$

compute the vertex observer gains in (12):

$$\mathcal{K}_i = P^{-1} M_i, \tag{24}$$

and choose the nonlinear function $\varphi(\hat{\rho})$ as:

$$\varphi(\hat{\rho}) = \begin{cases} 0 & \text{if } \bar{e}_y(t)^T \bar{e}_y(t) < \epsilon \\ \mu_3 \zeta_1(\hat{\rho})^2 \frac{\hat{\bar{X}}(t)^T \hat{\bar{X}}(t)}{2\bar{e}_y(t)^T \bar{e}_y(t)} P^{-1} C^T \bar{e}_y(t) + \mu_5 \frac{u(t)^T u(t)}{2\bar{e}_y(t)^T \bar{e}_y(t)} P^{-1} C^T \bar{e}_y(t) + \mu_7 \frac{K_s(\hat{\rho})^T K_s(\hat{\rho})}{2\bar{e}_y(t)^T \bar{e}_y(t)} P^{-1} C^T \bar{e}_y(t) & \text{if } \bar{e}_y(t)^T \bar{e}_y(t) \geq \epsilon \end{cases} \tag{25}$$

where:

$$\bar{e}_y(t) = \bar{Y}(t) - \hat{\bar{Y}}(t), \quad \mu_3 = \frac{1}{\mu_2 \mu_4}, \quad \mu_7 = \frac{\mu_8}{1 - \mu_2 \mu_8 (\mu_4 + 1)},$$

with μ_4 and ϵ arbitrarily chosen positive scalars. Then, the estimation error (19) is asymptotically stable with $\mathcal{H}_\infty$ performance and attenuation level $\gamma > 0$.

Proof Requiring (22) is equivalent to[19]:

$$\mathcal{J}(t) := \dot{V}(t) + \xi(t)^T \xi(t) - \gamma^2 v(t)^T v(t) < 0, \tag{26}$$

where $V(t) = \bar{e}(t)^T P \bar{e}(t)$, with $P > 0$. Hence, by considering (19), the following inequality is obtained:

$$\begin{aligned} \mathcal{J}(t) :=& \bar{e}(t)^T \left[(\mathcal{A}(\hat{\rho}) - \mathcal{K}(\hat{\rho})\mathcal{C})^T P + P(\mathcal{A}(\hat{\rho}) - \mathcal{K}(\hat{\rho})\mathcal{C}) \right] \bar{e}(t) + \mathcal{J}_a(t) + \mathcal{J}_b(t) + \mathcal{J}_c(t) + \mathcal{J}_d(t) \\ &+ \bar{e}(t)^T P W(\hat{\rho}) v(t) + v(t)^T W(\hat{\rho})^T P \bar{e}(t) - 2\bar{e}(t)^T P \varphi(\hat{\rho}) + \bar{e}(t)^T L^T L \bar{e}(t) - \gamma^2 v(t)^T v(t) < 0. \end{aligned} \tag{27}$$

where:

$$\mathcal{J}_a(t) = \bar{X}(t)^T \Delta\mathcal{A}(\hat{\rho})^T P \bar{e}(t) + \bar{e}(t)^T P \Delta\mathcal{A}(\hat{\rho}) \bar{X}(t), \tag{28}$$

$$\mathcal{J}_b(t) = u(t)^T \Delta\mathcal{B}(\hat{\rho})^T P \bar{e}(t) + \bar{e}(t)^T P \Delta\mathcal{B}(\hat{\rho}) u(t), \tag{29}$$

$$\mathcal{J}_c(t) = w(t)^T \Delta G(\hat{\rho})^T P \bar{e}(t) + \bar{e}(t)^T P \Delta G(\hat{\rho}) w(t), \tag{30}$$

$$\mathcal{J}_d(t) = K_s(\hat{\rho})^T P \bar{e}(t) + \bar{e}(t)^T P K_s(\hat{\rho}). \tag{31}$$

Using Lemma 1, we obtain:

$$\mathcal{J}_a(t) \leq \mu_1^{-1} (P\bar{e}(t))^T P \bar{e}(t) + \mu_1 \bar{X}(t)^T \Delta\mathcal{A}(\hat{\rho})^T \Delta\mathcal{A}(\hat{\rho}) \bar{X}(t), \tag{32}$$

with $\mu_1 > 0$ and considering (16), the following relationship is established:

$$\mu_1^{-1} (P\bar{e}(t))^T P \bar{e}(t) + \mu_1 \bar{X}(t)^T \Delta\mathcal{A}(\hat{\rho})^T \Delta\mathcal{A}(\hat{\rho}) \bar{X}(t) \leq \mu_1^{-1} \bar{e}(t)^T P^2 \bar{e}(t) + \mu_1 \zeta_1(\hat{\rho})^2 \bar{X}(t)^T \bar{X}(t), \tag{33}$$

where $\bar{X}(t) = \bar{e}(t) + \hat{\bar{X}}(t)$. Then, (33) becomes:

$$\mu_1^{-1} \bar{e}(t)^T P^2 \bar{e}(t) + \mu_1 \zeta_1(\hat{\rho})^2 \bar{X}(t)^T \bar{X}(t) = \mu_1^{-1} \bar{e}(t)^T P^2 \bar{e}(t) + \mu_1 \zeta_1(\hat{\rho})^2 \left(\bar{e}(t)^T \bar{e}(t) + \hat{\bar{X}}(t)^T \bar{e}(t) + \bar{e}(t)^T \hat{\bar{X}}(t) + \hat{\bar{X}}(t)^T \hat{\bar{X}}(t) \right). \tag{34}$$

Applying Lemma 1 again, (34) can be rewritten as:

$$\begin{aligned} &\mu_1^{-1} \bar{e}(t)^T P^2 \bar{e}(t) + \mu_1 \zeta_1(\hat{\rho})^2 \left(\bar{e}(t)^T \bar{e}(t) + \hat{\bar{X}}(t)^T \bar{e}(t) + \bar{e}(t)^T \hat{\bar{X}}(t) + \hat{\bar{X}}(t)^T \hat{\bar{X}}(t) \right) \leq \mu_1^{-1} \bar{e}(t)^T P^2 \bar{e}(t) \\ &+ \mu_2^{-1} \zeta_1(\hat{\rho})^2 \bar{e}(t)^T \bar{e}(t) + \mu_3 \zeta_1(\hat{\rho})^2 \hat{\bar{X}}(t)^T \hat{\bar{X}}(t), \end{aligned} \tag{35}$$

where $\mu_2^{-1} = \mu_1(1 + \mu_4)$ and $\mu_3 = \mu_1(1 + \mu_4^{-1})$, with $\mu_4 > 0$.

Following a similar reasoning and taking into account (17)-(18), we obtain:

$$\mathcal{J}_b(t) \leq \mu_5^{-1} \bar{e}(t)^T P \Delta\mathcal{B}(\hat{\rho}) \Delta\mathcal{B}(\hat{\rho})^T P \bar{e}(t) + \mu_5 u(t)^T u(t) \leq \mu_5^{-1} \zeta_2(\hat{\rho})^2 \bar{e}(t)^T P^2 \bar{e}(t) + \mu_5 u(t)^T u(t), \tag{36}$$

$$\mathcal{J}_c(t) \leq \mu_6^{-1} \bar{e}(t)^T P \Delta G(\hat{\rho}) \Delta G(\hat{\rho})^T P \bar{e}(t) + \mu_6 w(t)^T w(t) \leq \mu_6^{-1} \zeta_3(\hat{\rho})^2 \bar{e}(t)^T P^2 \bar{e}(t) + \mu_6 w(t)^T w(t), \tag{37}$$

$$\mathcal{J}_d(t) \leq \mu_7^{-1} \bar{e}(t)^T P^2 \bar{e}(t) + \mu_7 K_s(\hat{\rho})^T K_s(\hat{\rho}). \tag{38}$$

with $\mu_5,\ \mu_6,\ \mu_7 > 0$.

Since the subsystems of the augmented system in (11) are observable, if $\bar{e}_y(t)$ is zero, the estimation error is zero, therefore $\varphi(\hat{\rho}) = 0$. If $\bar{e}_y(t)$ is non-zero, in order to cancel the effect of the uncertainties on the dynamics of the output system, $\varphi(\hat{\rho})$ is selected as in Equation (25), such that:

$$\begin{aligned}2\bar{e}(t)^T P\varphi(\hat{\rho}) =& 2\bar{e}(t)^T P\mu_3\zeta_1(\hat{\rho})^2\frac{\hat{\bar{X}}(t)^T\hat{\bar{X}}(t)}{2\bar{e}_y(t)^T\bar{e}_y(t)}P^{-1}C^T\bar{e}_y(t) + 2\bar{e}(t)^T P\mu_5\frac{u(t)^T u(t)}{2\bar{e}_y(t)^T\bar{e}_y(t)}P^{-1}C^T\bar{e}_y(t)\\ &+ 2\bar{e}(t)^T P\mu_7\frac{K_s(\hat{\rho})^T K_s(\hat{\rho})}{2\bar{e}_y(t)^T\bar{e}_y(t)}P^{-1}C^T\bar{e}_y(t)\\ =&\left(\mu_3\zeta_1(\hat{\rho})^2\hat{\bar{X}}(t)^T\hat{\bar{X}}(t) + \mu_5 u(t)^T u(t) + \mu_7 K_s(\hat{\rho})^T K_s(\hat{\rho})\right)\frac{2\bar{e}(t)^T P}{2\bar{e}_y(t)^T\bar{e}_y(t)}P^{-1}C^T\bar{e}_y(t)\end{aligned}$$

considering that $\bar{e}_y(t) = C\bar{e}(t)$:

$$\begin{aligned}2\bar{e}(t)^T P\varphi(\hat{\rho}) =& \left(\mu_3\zeta_1(\hat{\rho})^2\hat{\bar{X}}(t)^T\hat{\bar{X}}(t) + \mu_5 u(t)^T u(t) + \mu_7 K_s(\hat{\rho})^T K_s(\hat{\rho})\right)\frac{2\bar{e}(t)^T PP^{-1}C^T C\bar{e}(t)}{2\bar{e}(t)^T C^T C\bar{e}(t)}\\ =&\mu_3\zeta_1(\hat{\rho})^2\hat{\bar{X}}(t)^T\hat{\bar{X}}(t) + \mu_5 u(t)^T u(t) + \mu_7 K_s(\hat{\rho})^T K_s(\hat{\rho}),\end{aligned} \tag{39}$$

Hence, taking into account (35)-(39), (27) leads to:

$$\mathcal{J}(t) \leq \bar{e}(t)^T\Gamma(\hat{\rho})\bar{e}(t) + \bar{e}(t)^T PW(\hat{\rho})v(t) + v(t)^T W(\hat{\rho})^T P\bar{e}(t) + \mu_6 w(t)^T w(t) - \gamma^2 v(t)^T v(t) < 0, \tag{40}$$

where:

$$\Gamma(\hat{\rho}) = (\mathcal{A}(\hat{\rho}) - \mathcal{K}(\hat{\rho})C)^T P + P(\mathcal{A}(\hat{\rho}) - \mathcal{K}(\hat{\rho})C) + \mu_8^{-1}P^2 + \mu_2^{-1}\zeta_1(\hat{\rho})^2 I + \mu_5^{-1}\zeta_2(\hat{\rho})^2 P^2 + \mu_6^{-1}\zeta_3(\hat{\rho})^2 P^2 + L^T L, \tag{41}$$

and $\mu_8^{-1} = \mu_1^{-1} + \mu_7^{-1}$, then using (20), (40) can be rewritten in a compact matrix form as follows:

$$\begin{bmatrix}\bar{e}(t)^T & f_k(t)^T & w(t)^T\end{bmatrix}\begin{bmatrix}\Gamma(\hat{\rho}) & PR & PG(\hat{\rho})\\ R^T P & -\gamma^2 I & 0\\ G(\hat{\rho})^T P & 0 & (\mu_6 - \gamma^2)I\end{bmatrix}\begin{bmatrix}\bar{e}(t)\\ f_k(t)\\ w(t)\end{bmatrix} < 0 \tag{42}$$

which holds if:

$$\begin{bmatrix}\Gamma(\hat{\rho}) & PR & PG(\hat{\rho})\\ R^T P & -\gamma^2 I & 0\\ G(\hat{\rho})^T P & 0 & (\mu_6 - \gamma^2)I\end{bmatrix} < 0 \tag{43}$$

Since (43) is nonlinear, due to the product between decision variables $\mathcal{K}(\hat{\rho})$ and P, the change of variable $M(\hat{\rho}) = P\mathcal{K}(\hat{\rho})$ is needed to obtain an LMI representation. Finally, by taking into account (2) and applying Schur complements, (23) is obtained from (43), thus completing the proof.

In a practical implementation of the proposed technique, as the estimation error $\bar{e}_y(t)$ approaches to zero, the value of $\varphi(\hat{\rho})$ will increase without limit. One can overcome this problem by considering a small region in the neighborhood of zero defined by a small positive scalar ϵ where $\bar{e}_y(t)$ is kept, as pointed out in Theorem 1.

4 | FAULT DIAGNOSIS OF AN OCTOROTOR UNMANNED AERIAL VEHICLE

In this section, the proposed methodology for actuator and sensor fault estimation is applied to an octorotor UAV and it is validated using simulation results. The considered actuator faults are losses of effectiveness in the UAV's motors.

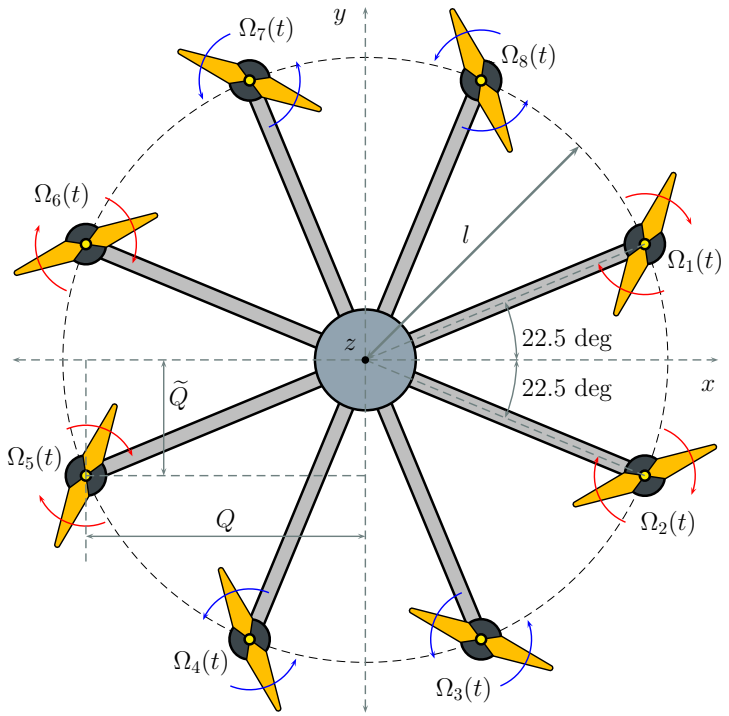

FIGURE 2 Star-shaped octorotor configuration

Figure 2 shows the configuration of the octorotor UAV considered in this paper whose dynamics are described by the following equations:[41]

$$\text{Translational part}\begin{cases}\ddot{x}_b(t) = & (\cos\phi(t)\sin\theta(t)\cos\psi(t) + \sin\phi(t)\sin\psi(t))\dfrac{1}{m}u_f(t)\\ \ddot{y}_b(t) = & (\cos\phi(t)\sin\theta(t)\sin\psi(t) + \sin\phi(t)\cos\psi(t))\dfrac{1}{m}u_f(t)\\ \ddot{z}_b(t) = & -g + \cos\phi(t)\sin\theta(t)\dfrac{1}{m}u_f(t)\end{cases} \tag{44}$$

$$\text{Rotational part}\begin{cases}\ddot{\psi}(t) = & \dot{\theta}(t)\dot{\psi}(t)\left(\dfrac{I_y - I_z}{I_x}\right) - \dfrac{I_r}{I_x}\dot{\theta}(t)\Omega(t) + \dfrac{1}{I_x}\tau_\phi(t)\\ \ddot{\theta}(t) = & \dot{\phi}(t)\dot{\psi}(t)\left(\dfrac{I_z - I_x}{I_y}\right) + \dfrac{I_r}{I_y}\dot{\psi}(t)\Omega(t) + \dfrac{1}{I_y}\tau_\theta(t)\\ \ddot{\psi}(t) = & \dot{\phi}(t)\dot{\theta}(t)\left(\dfrac{I_x - I_y}{I_z}\right) + \dfrac{1}{I_z}\tau_\psi(t)\end{cases} \tag{45}$$

where $x_b(t)$, $y_b(t)$, $z_b(t)$ and $\dot{x}_b(t)$, $\dot{y}_b(t)$, $\dot{z}_b(t)$ define the position and velocity of the translation of the octorotor, $\phi(t)$ is the roll angle, $\theta(t)$ is the pitch angle, $\psi(t)$ is the yaw angle, $\dot{\phi}(t)$, $\dot{\theta}(t)$, $\dot{\psi}(t)$ are the angular velocities, $\Omega(t)$ is the disturbance caused by the residual of overall rotor speed, defined as:

$$\Omega(t) = -\Omega_1(t) - \Omega_2(t) + \Omega_3(t) + \Omega_4(t) - \Omega_5(t) - \Omega_6(t) + \Omega_7(t) + \Omega_8(t), \tag{46}$$

and $u_f(t)$ is the total thrust, $\tau_\phi(t)$, $\tau_\theta(t)$ and $\tau_\psi(t)$ are the torques, defined as:

$$\begin{aligned}u_f(t) =& F_1(t) + F_2(t) + F_3(t) + F_4(t) + F_5(t) + F_6(t) + F_7(t) + F_8(t),\\ \tau_\phi(t) =& Q\big(F_7(t) + F_8(t) - F_3(t) - F_4(t)\big) + \widetilde{Q}\big(F_1(t) + F_6(t) - F_2(t) - F_5(t)\big),\\ \tau_\theta(t) =& Q\big(F_5(t) + F_6(t) - F_1(t) - F_2(t)\big) + \widetilde{Q}\big(F_4(t) + F_7(t) - F_3(t) - F_8(t)\big),\\ \tau_\psi(t) =& \tau_3(t) + \tau_4(t) + \tau_7(t) + \tau_8(t) - \tau_1(t) - \tau_2(t) - \tau_5(t) - \tau_6(t),\end{aligned} \tag{47}$$

with:

$$F_i(t) = b \cdot \Omega_i^2(t), \tag{48}$$

$$\tau_i(t) = d \cdot \Omega_i^2(t), \quad \text{for } i = 1, \dots, 8, \tag{49}$$

where $\Omega_i(t)$, $i = 1, \dots, 8$ are the angular speeds of the rotors, $Q = l\cos(\pi/8)$ and $\widetilde{Q} = l\sin(\pi/8)$, l are the arm lengths, m is the total mass, I_x, I_y, and I_z are the inertia on the x, y, and z axis, respectively, b is the thrust coefficient, d is the drag coefficient, I_r is the inertia of the motor, and g is the gravitational acceleration. The nominal parameters used for the simulations are listed in Table 1.

TABLE 1 Parameter values used in the simulations

Parameter	value	unit	Parameter	value	unit	Parameter	value	unit
l	0.4	m	b	10×10^{-6}	N s^2	I_x	0.044	kg m^2
m	1.64	kg	d	0.3×10^{-6}	N m s^2	I_y	0.044	kg m^2
g	9.81	m/s^2	I_r	90×10^{-6}	kg m^2	I_z	0.088	kg m^2

Remark 1. The octorotor UAV is inherently unstable; for this reason, a controller is necessary to stabilize this system. An altitude controller will calculate $u_f(t)$ to get the total thrust. The $x-y$ position controller will calculate the desired pitch and roll angles depending on the desired values for x and y. These angles, along with the desired yaw angle, are inputs to the attitude controller which provides $\tau_\phi(t)$, $\tau_\theta(t)$ and $\tau_\psi(t)$. A sliding mode control (SMC), developed in the work of Adir and Stoica[42], has been chosen to stabilize the system for its characteristics of robustness to disturbances and uncertainty. Also, according to the works of Li et al.[43], Wang et tal.[44] and Saied et al.[45] the SMC can be used as a passive fault-tolerant control since it can maintain the stability of the system under certain faults. It is important to note that the proposed work is not dedicated to analyzing the controller, but the fault diagnosis method. Therefore, for more information about the FTC, the reader should refer to the cited works.

4.1 | LPV model of the octorotor

The dynamics of the octorotor UAV can be separated into two subsystems: the translational part and the rotational part, as it can be seen in (44) and (45). It is well known that the attitude dynamics is much faster than the translational one. Moreover, the attitude dynamics is decoupled of the translational dynamics. Nevertheless, the translational dynamics is related with the attitude dynamics. Thus, it is possible to separate the system into two independent subsystems.[46] Because it is assumed that the vehicle is flying in a hover position and actuator faults are considered, only the rotational dynamics of the UAV is used for the design of the fault diagnosis system.[47,48,49,50] The corresponding differential equations (45) can be reshaped into a quasi-LPV structure, as follows:

$$\dot{x}(t) = A(\rho_1(t), \rho_2(t))x(t) + Bu(t) + F_a(\rho_1(t), \rho_2(t))f_a(t) + J(\rho_1(t), \rho_2(t))w(t), \tag{50}$$

where:

$$x(t) = \left[\, \phi(t)\ \theta(t)\ \psi(t)\ \dot{\phi}(t)\ \dot{\theta}(t)\ \dot{\psi}(t) \,\right]^T = \left[\, x_1(t)\ x_2(t)\ x_3(t)\ x_4(t)\ x_5(t)\ x_6(t) \,\right]^T, \tag{51}$$

$$u(t) = \left[\, \tau_\phi(t)\ \tau_\theta(t)\ \tau_\psi(t) \,\right]^T, \tag{52}$$

and the exogenous disturbances/noise vector is $w(t) = \left[\, \Omega(t)\ w_n(t) \,\right]^T$, with $\Omega(t)$ denoting the disturbances and $w_n(t)$ the noise, respectively.

By defining $\rho_1(t) = x_4(t)$ and $\rho_2(t) = x_5(t)$, the matrices $A(\cdot)$, B and $J(\cdot)$ are defined as:

$$A(\rho_1(t),\rho_2(t)) = \begin{bmatrix} 0&0&0&1&0&0\\ 0&0&0&0&1&0\\ 0&0&0&0&0&1\\ 0&0&0&0&0&c_1\rho_2(t)\\ 0&0&0&0&0&c_2\rho_1(t)\\ 0&0&0&c_3\rho_2(t)&0&0 \end{bmatrix}, \quad B = \begin{bmatrix} 0&0&0\\ 0&0&0\\ 0&0&0\\ c_4&0&0\\ 0&c_5&0\\ 0&0&c_6 \end{bmatrix}, \quad J(\rho_1(t),\rho_2(t)) = \begin{bmatrix} 0&0\\ 0&0\\ 0&0\\ -c_7\rho_2(t)&0\\ c_8\rho_1(t)&0\\ 0&0 \end{bmatrix}, \tag{53}$$

with constants $c_1 = (I_y - I_z)/I_x$, $c_2 = (I_z - I_x)/(I_y)$, $c_3 = (I_x - I_y)/I_z$), $c_4 = 1/I_x$, $c_5 = 1/I_y$, $c_6 = 1/I_z$, $c_7 = I_r/I_x$ and $c_8 = I_r/I_y$.

By considering $\rho(t) = [\rho_1(t),\ \rho_2(t)]^T$ as the scheduling variables vector with $\rho_1(t) \in [\rho_{1min}\quad \rho_{1max}] = [-2\quad 2]$ rad/s, $\rho_2(t) \in [\rho_{2min}\quad \rho_{2max}] = [-3\quad 3]$ rad/s, the quasi-LPV system (50) can be rewritten into a polytopic representation using the nonlinear sector transformation,[51] as follows:

$$\dot{x}(t) = \sum_{i=1}^{4} \alpha_i(\rho(t))\Big(A_i x(t) + Bu(t) + F_{a,i} f_a(t) + J_i w(t)\Big) \tag{54}$$

where the weighting functions are defined as:

$$\begin{aligned} \alpha_1(\rho(t)) &= \frac{\rho_1(t) - \rho_{1min}}{\rho_{1max} - \rho_{1min}} \frac{\rho_2(t) - \rho_{2min}}{\rho_{2max} - \rho_{2min}},\\ \alpha_2(\rho(t)) &= \frac{\rho_1(t) - \rho_{1min}}{\rho_{1max} - \rho_{1min}} \frac{\rho_{2max} - \rho_2(t)}{\rho_{2max} - \rho_{2min}}, \end{aligned} \tag{55}$$

$$\begin{aligned} \alpha_3(\rho(t)) &= \frac{\rho_{1max} - \rho_1(t)}{\rho_{1max} - \rho_{1min}} \frac{\rho_2(t) - \rho_{2min}}{\rho_{2max} - \rho_{2min}},\\ \alpha_4(\rho(t)) &= \frac{\rho_{1max} - \rho_1(t)}{\rho_{1max} - \rho_{1min}} \frac{\rho_{2max} - \rho_2(t)}{\rho_{2max} - \rho_{2min}}, \end{aligned} \tag{56}$$

with $A_1 = A(\rho_{1max}, \rho_{2max})$, $A_2 = A(\rho_{1max}, \rho_{2min})$, $A_3 = A(\rho_{1min}, \rho_{2max})$, $A_4 = A(\rho_{1min}, \rho_{2min})$, $J_1 = J(\rho_{1max}, \rho_{2max})$, $J_2 = J(\rho_{1max}, \rho_{2min})$, $J_3 = J(\rho_{1min}, \rho_{2max})$, $J_4 = J(\rho_{1min}, \rho_{2min})$. In the following section, $F_{a,i}$ and $f_a(t)$ are characterized.

4.2 | Actuator and sensor faults on the octorotor system

In order to consider the presence of actuator faults, the losses of effectiveness are represented by:

$$N(t) = \begin{bmatrix} N_1(t)\ N_2(t)\ \dots\ N_8(t) \end{bmatrix}^T \tag{57}$$

where $N_1(t), \dots, N_8(t)$ represent the level of effectiveness of each rotor. In particular, $N_j(t) = 0$ means that the rotor j is working without fault, whereas $0 < N_j(t) < 1$ means that the rotor j has a partial fault and, as a consequence, the corresponding actuator operates with reduced capacity. If $N_j(t) = 1$, then the rotor j is undergoing a total fault.
The thrust and torque produced by a faulty rotor are described by:

$$\begin{aligned} \widetilde{F}_i(t) &= (1 - N_i(t))F_i(t),\\ \widetilde{\tau}_i(t) &= (1 - N_i(t))\tau_i(t), \end{aligned} \tag{58}$$

then, the loss of efficiency in a rotor appears as an additive fault on the control inputs of the system ($\tau_\phi(t)$, $\tau_\theta(t)$ and $\tau_\psi(t)$), which can be isolated and estimated by means of a fault diagnosis scheme. It is important to emphasize that it is possible to approximate the loss of efficiency through an additive representation if and only if the fault occurrence does not cause instability.[52] Therefore, when a rotor fails, there appears a loss of thrust that generates positive or negative moments in the Euler angle directions,[53] which causes residual torques to occur in the input torques. In this situation, the real inputs $[\widetilde{\tau}_\phi(t)\ \ \widetilde{\tau}_\theta(t)\ \ \widetilde{\tau}_\psi(t)]^T$ applied to the system are unknown, so they can be described as follows:

$$\begin{bmatrix} \widetilde{\tau}_\phi(t)\\ \widetilde{\tau}_\theta(t)\\ \widetilde{\tau}_\psi(t) \end{bmatrix} = \begin{bmatrix} \tau_\phi(t)\\ \tau_\theta(t)\\ \tau_\psi(t) \end{bmatrix} + \begin{bmatrix} \Delta\tau_\phi(t)\\ \Delta\tau_\theta(t)\\ \Delta\tau_\psi(t) \end{bmatrix} \tag{59}$$

where $[\tau_\phi(t) \quad \tau_\theta(t) \quad \tau_\psi(t)]^T$ are the nominal inputs calculated by the controller and $f_a(t) = [\Delta\tau_\phi(t) \quad \Delta\tau_\theta(t) \quad \Delta\tau_\psi(t)]^T$ are the residual torques, that are considered to be faults for estimation purposes, in this case, $F_1 = F_2 = F_3 = F_4 = \boldsymbol{B}$. For example, when there is a loss of effectiveness in the rotor 1, the thrust is $\widetilde{F}_1(t) = (1 - N_1(t))F_1(t)$, and the torque is given by $\widetilde{\tau}_1(t) = (1 - N_1(t))\tau_1(t)$ so substituting these expressions in (47), the corresponding torques developed by the actuators are:

$$\begin{aligned}
\widetilde{\tau}_\phi(t) =& Q\big(F_7(t) + F_8(t) - F_3(t) - F_4(t)\big) + \widetilde{Q}\big((1 - N_1(t))F_1(t) + F_6(t) - F_2(t) - F_5(t)\big),\\
\widetilde{\tau}_\theta(t) =& Q\big(F_5(t) + F_6(t) - (1 - N_1(t))F_1(t) - F_2(t)\big) + \widetilde{Q}\big(F_4(t) + F_7(t) - F_3(t) - F_8(t)\big),\\
\widetilde{\tau}_\psi(t) =& \tau_3(t) + \tau_4(t) + \tau_7(t) + \tau_8(t) - (1 - N_1(t))\tau_1(t) - \tau_2(t) - \tau_5(t) - \tau_6(t),
\end{aligned} \tag{60}$$

and using (47), (60) can be expressed as:

$$\widetilde{\tau}_\phi(t) = \tau_\phi(t) - N_1(t)\widetilde{Q}F_1(t), \tag{61}$$

$$\widetilde{\tau}_\theta(t) = \tau_\theta(t) + N_1(t)QF_1(t), \tag{62}$$

$$\widetilde{\tau}_\psi(t) = \tau_\psi(t) + N_1(t)\tau_1(t). \tag{63}$$

Then, the residual torques are:

$$\Delta\tau_\phi(t) = -N_1(t)\widetilde{Q}F_1(t), \tag{64}$$

$$\Delta\tau_\theta(t) = +N_1(t)QF_1(t), \tag{65}$$

$$\Delta\tau_\psi(t) = +N_1(t)\tau_1(t). \tag{66}$$

Generalizing to the other rotors, the corresponding torques provided by the actuators are:

$$\begin{cases} \widetilde{\tau}_\phi(t) = \tau_\phi(t) \pm N_i(t)QF_i(t), \\ \widetilde{\tau}_\theta(t) = \tau_\theta(t) \pm N_i(t)\widetilde{Q}F_i(t), \end{cases} \text{for } \; i = 3, 4, 7, 8 \tag{67}$$

$$\begin{cases} \widetilde{\tau}_\phi(t) = \tau_\phi(t) \pm N_i(t)\widetilde{Q}F_i(t), \\ \widetilde{\tau}_\theta(t) = \tau_\theta(t) \pm N_i(t)QF_i(t), \end{cases} \text{for } \; i = 1, 2, 5, 6 \tag{68}$$

$$\widetilde{\tau}_\psi(t) = \tau_\psi(t) \pm N_i(t)\tau_i(t), \;\; \text{for } \; i = 1, \ldots, 8 \tag{69}$$

then:

$$\begin{cases} \Delta\tau_\phi(t) = \pm N_i(t)QF_i(t), \\ \Delta\tau_\theta(t) = \pm N_i(t)\widetilde{Q}F_i(t), \end{cases} \text{for } \; i = 3, 4, 7, 8 \tag{70}$$

$$\begin{cases} \Delta\tau_\phi(t) = \pm N_i(t)\widetilde{Q}F_i(t), \\ \Delta\tau_\theta(t) = \pm N_i(t)QF_i(t), \end{cases} \text{for } \; i = 1, 2, 5, 6 \tag{71}$$

$$\Delta\tau_\psi(t) = \pm N_i(t)\tau_i(t), \text{for } \; i = 1, \ldots, 8 \tag{72}$$

where the actual sign represented by the symbol $\pm$ depends on the considered torque and motor, as summarized in Table 2.

TABLE 2 Additive faults according to the failing motor

Fault	$\Delta\tau_\phi(t)$	$\Delta\tau_\theta(t)$	$\Delta\tau_\psi(t)$	Fault	$\Delta\tau_\phi(t)$	$\Delta\tau_\theta(t)$	$\Delta\tau_\psi(t)$
Motor 1	−	+	+	Motor 5	+	−	+
Motor 2	+	+	+	Motor 6	−	−	+
Motor 3	+	+	−	Motor 7	−	−	−
Motor 4	+	−	−	Motor 8	−	+	−

Using Table 2, the fault of a rotor can be isolated, and then using the information on the nominal angular speed of the rotor calculated by the controller, and by the equations (70), (71) or (72), the efficiency can be estimated. In this work, it is considered that the octorotor is equipped with sensors that measure the angular positions $\phi(t)$, $\theta(t)$ and $\psi(t)$, and the angular velocities

$\dot{\phi}(t)$, $\dot{\theta}(t)$. Also, two additive sensor faults $f_s(t)$ are considered affecting the angular positions $\phi(t)$ and $\theta(t)$. Hence, the output equation is defined as follows:

$$y(t) = Cx(t) + F_s f_s(t) + Dw(t), \tag{73}$$

where:

$$C = \begin{pmatrix} 1 & 0 & 0 & 0 & 0 & 0 \\ 0 & 1 & 0 & 0 & 0 & 0 \\ 0 & 0 & 1 & 0 & 0 & 0 \\ 0 & 0 & 0 & 1 & 0 & 0 \\ 0 & 0 & 0 & 0 & 1 & 0 \end{pmatrix}, \qquad F_s = \begin{bmatrix} 1 & 0 \\ 0 & 1 \\ 0 & 0 \\ 0 & 0 \\ 0 & 0 \end{bmatrix}, \qquad D = \begin{bmatrix} 0 & 1 \\ 0 & 1 \\ 0 & 1 \\ 0 & 1 \\ 0 & 1 \end{bmatrix}.$$

Solving the LMI (23) of Theorem 1, the unknown gains of the PMISMO are obtained. The constants are selected as $E = 30$, $\epsilon = 10^{-1}$, $\mu_4 = 0.1$ and since the main objective is to estimate the faults the matrix L is chosen as:

$$L = \begin{bmatrix} 0_{5\times6} & 0_{5\times5} & I_{5\times5} & 0_{5\times5} \end{bmatrix}. \tag{74}$$

In this case, to consider a 10% uncertainty in the weight functions, the uncertain factors are bounded as follows:

$$\lambda_i \in [0.9 \;\; 1.1], \text{ for } i = 1, \ldots, 4, \tag{75}$$

and it is possible to compute $\zeta_{1,i}$, $\zeta_{2,i}$ and $\zeta_{3,i}$ from (13), (14) and (15), respectively, whose values are found in the Appendix.

The simulation results are carried out with an attenuation level $\gamma = 0.23$, the obtained constants $\mu_2 = 32.6039$, $\mu_5 = 11.3383$, $\mu_6 = 0.0480$, $\mu_8 = 0.0011$ and matrices K_i $(i = 1, \ldots, 4)$, whose values can be found in the Appendix, are used to implement the PMISMO (12) whose performance is validated by simulations.

The initial conditions of the rotational part of the system is:

$$x_0 = [\, 0 \;\; 0 \;\; 0 \;\; 0 \;\; 0 \;\; 0 \,]^T, \tag{76}$$

the initial conditions for the PMISMO is:

$$\hat{\hat{X}}_0 = 0_{21\times1}, \tag{77}$$

and for the filter is:

$$z_0 = [\, 0.01 \;\; 0.01 \;\; 0.01 \;\; 0.01 \;\; 0.01 \,]^T. \tag{78}$$

The measurement noise $w(t)$ in the output is a band-limited white noise, with noise power 1×10^{-6}. The system outputs, the filtered signals and the estimates are shown in Figure 3 and Figure 4.

For a more realistic scenario, the scheduling variables applied to the NLPV PMISMO are obtained from the measurements of $y_4(t) = \dot{\phi}(t)$ and $y_5(t) = \dot{\theta}(t)$, which are affected by measurement noise. The uncertainty weighting functions that depend on the scheduling variables are shown in Figure 5. In this case, the measurements of the scheduling variables are considered to be fault-free.

To demonstrate the effectiveness of the observer to estimate actuator faults, a time-varying fault has been induced in rotor 2, which causes a maximum loss of 50% in the efficiency of the rotor from $t = 10$s to $t = 60$s approximately, which causes residual torques in the system that are estimated by the NLPV PMISMO. The signals $\Delta\tau_\phi(t)$, $\Delta\tau_\theta(t)$, $\Delta\tau_\psi(t)$ and their estimations are shown in Figure 6, and their signs are compared with the values of Table 2 in order to isolate the actuator fault. In this case, the fault in the rotor is considered to be a time-varying signal with a norm-bounded second-derivative. By knowing the nominal values of the motors speeds calculated by the controller and using either equations (70), (71) or (72), the efficiency of the rotor is reconstructed. The loss of efficiency in rotor 2 and its estimation are shown in Figure 7.

To verify the effectiveness of the NLPV PMISMO to estimate sensor faults, two time-varying faults are induced: $f_{s_1}(t)$ is the fault on the sensor that measures the angular position $\phi(t)$ from $t = 20$s to $t = 70$s and $f_{s_2}(t)$ is the fault on the sensor that measures the angular position $\theta(t)$ from $t = 30$ to $t = 80$s, both faults are time-varying signals with maximum magnitudes of 0.25. Figure 8 shows the sensor fault and its estimation. As it can be seen, the time lapses in which the two faults occur are overlapping, which allows verifying the efficiency of the proposed observer in the event of simultaneous faults. The fault estimation turns out to be successful.

Figure 9 show that the state of the system is estimated correctly despite the actuator and sensor faults and the measurement noise that affects the output and the scheduling variables.

The obtained results demonstrate that the proposed NLPV PMISMO has a good performance for the estimation of actuators and sensors faults in LPV systems with uncertain scheduling variables.

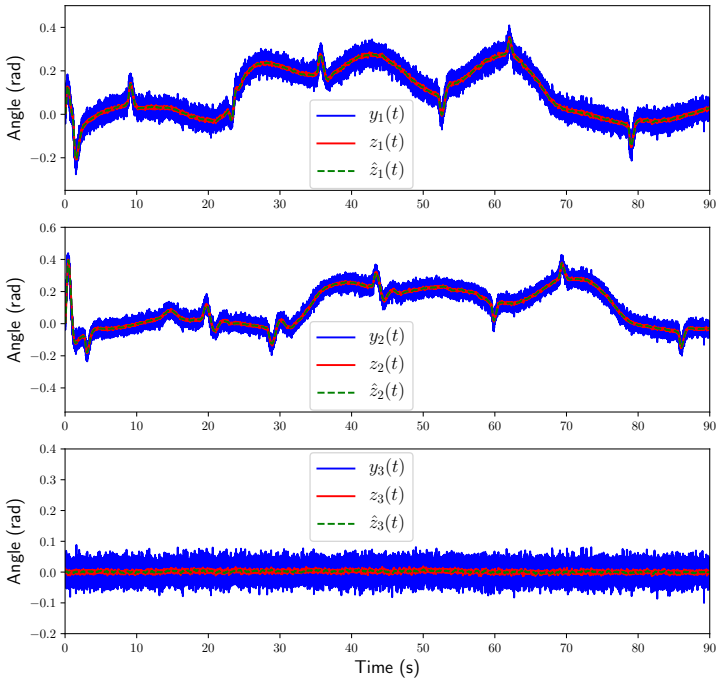

FIGURE 3 Measured angular positions $y_1(t)$, $y_2(t)$ and $y_3(t)$, their filtered versions $z_1(t)$, $z_2(t)$ and $z_3(t)$, and the estimate signals $\hat{z}_1(t)$, $\hat{z}_2(t)$ and $\hat{z}_3(t)$.

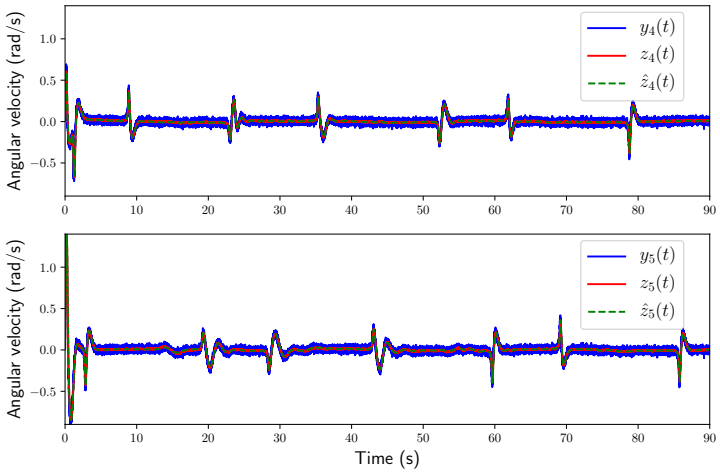

FIGURE 4 Measured angular velocities $y_4(t)$ and $y_5(t)$, their filtered signals $z_4(t)$ and $z_5(t)$, and the estimates $\hat{z}_4(t)$ and $\hat{z}_5(t)$.

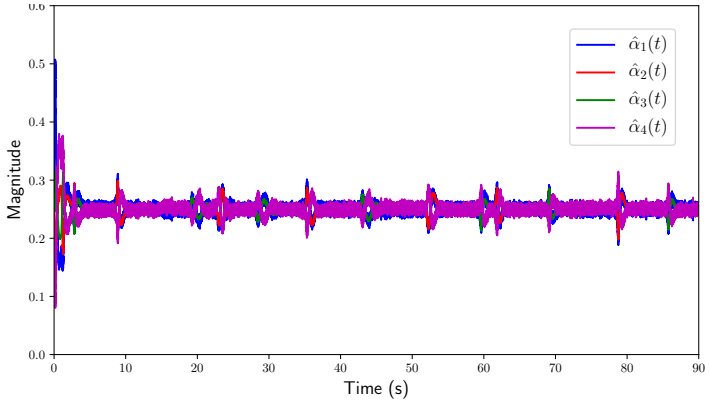

FIGURE 5 Inexact weighting functions.

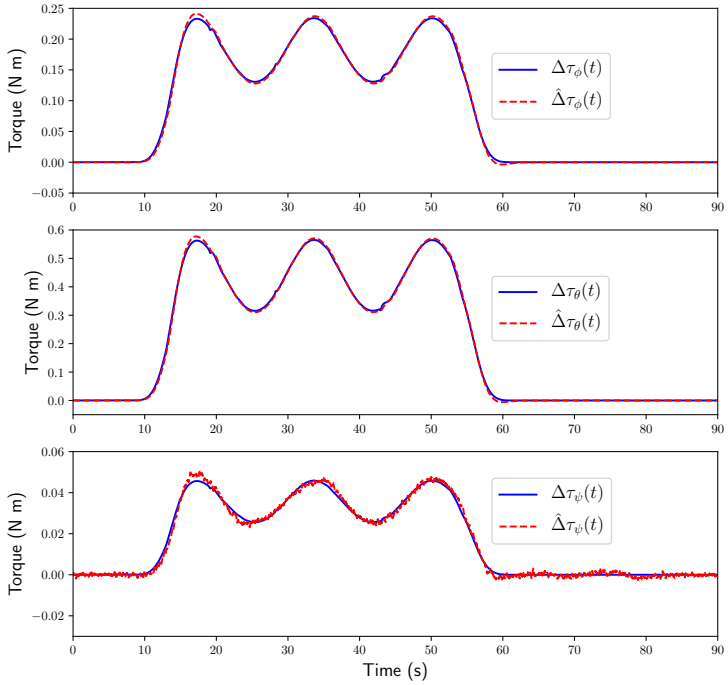

FIGURE 6 Signals $\Delta\tau_\phi(t)$, $\Delta\tau_\theta(t)$, $\Delta\tau_\psi(t)$ and their estimates.

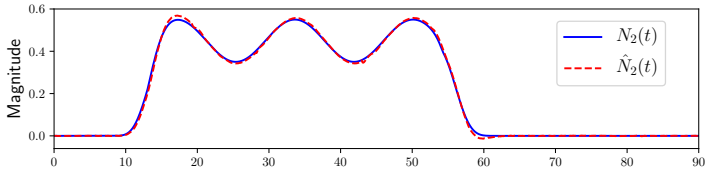

FIGURE 7 Rotor efficiency with partial fault and its estimate

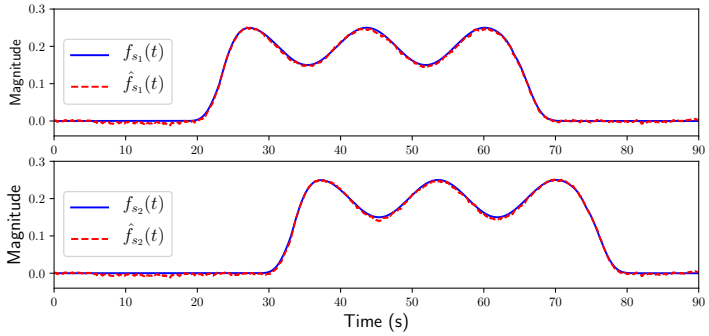

FIGURE 8 Sensor faults and their estimates

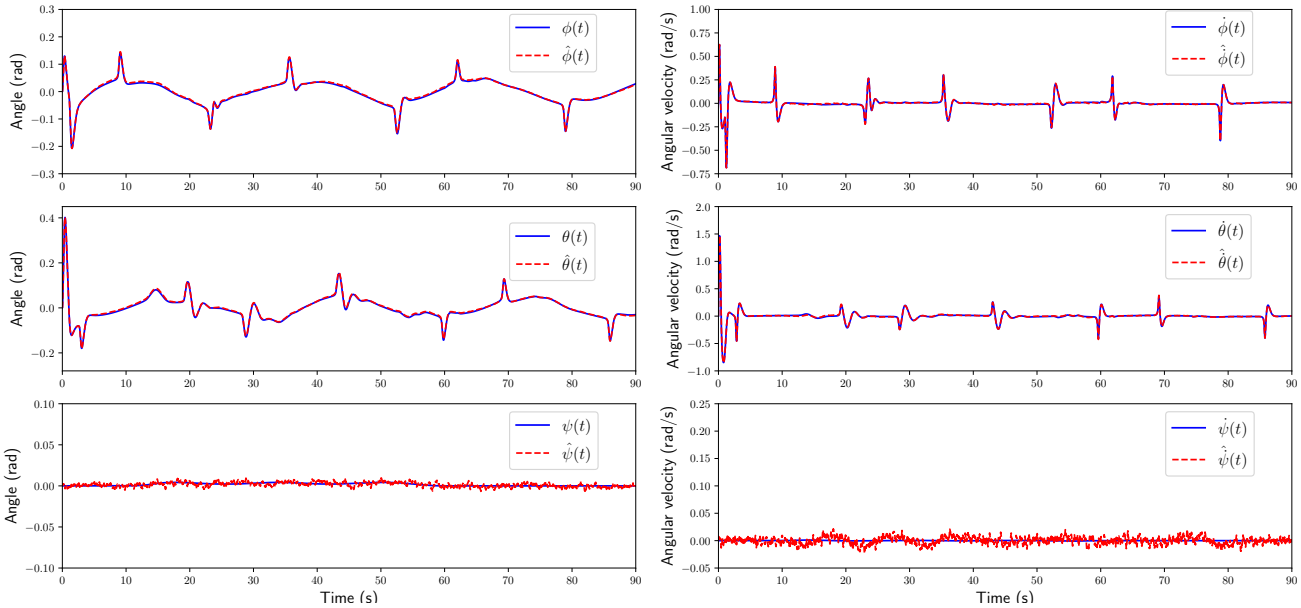

FIGURE 9 State variables and their estimates.

5 | CONCLUSIONS

This paper dealt with the estimation of system states, sensors and actuator faults in nonlinear systems described by LPV models affected by noisy measurements in the scheduling variables and system outputs. A proportional multiple-integral sliding mode observer was designed with a $\mathcal{H}_\infty$ performance criterion in order to guarantee stability and robustness against the sensor noise and the uncertainty induced by inexact scheduling variables. Finally, the developed observer was applied in a physical system consisting of an octorotor UAV system in order to show the applicability and effectiveness of the proposed approach. It was

demonstrated that the proposed approach allows estimating simultaneously states and faults with good performance. There are different research paths that could be explored next, for instance, the authors will work in integrating the method with fault-tolerant control techniques. Based on the computed fault estimation, a reconfigurable control scheme can be developed with the aim of maintaining an acceptable performance and close-to-nominal steady-state of the system under fault occurrence.

References

1. Chen L, Alwi H, Edwards C. Development and evaluation of an integral sliding mode fault-tolerant control scheme on the RECONFIGURE benchmark. *International Journal of Robust and Nonlinear Control* 2019; 29(16): 5314–5340.

2. Gómez-Peñate S, Valencia-Palomo G, López-Estrada FR, Astorga-Zaragoza CM, Osornio-Rios RA, Santos-Ruiz I. Sensor fault diagnosis based on a sliding mode and unknown input observer for Takagi-Sugeno systems with uncertain premise variables. *Asian Journal of Control* 2019; 21(1): 339–353.

3. Alwi H, Edwards C, Marcos A. Fault reconstruction using a LPV sliding mode observer for a class of LPV systems. *Journal of the Franklin Institute* 2012; 349(2): 510–530.

4. Henry D, Cieslak J, Zolghadri A, Efimov D. $\mathcal{H}_\infty/\mathcal{H}_-$ LPV solutions for fault detection of aircraft actuator faults: Bridging the gap between theory and practice. *International Journal of Robust and Nonlinear Control* 2015; 25(5): 649–672.

5. Jia Q, Chen W, Zhang Y, Chen X. Robust fault reconstruction via learning observers in linear parameter-varying systems subject to loss of actuator effectiveness. *IET Control Theory & Applications* 2014; 8(1): 42–50.

6. Guzmán-Rabasa JA, López-Estrada FR, González-Contreras BM, Valencia-Palomo G, Chadli M, Pérez-Patricio M. Actuator fault detection and isolation on a quadrotor unmanned aerial vehicle modeled as a linear parameter-varying system. *Measurement and Control* 2019; 52(9-10): 1228–1239.

7. Rotondo D, Cristofaro A, Johansen TA, Nejjari F, Puig V. Robust fault and icing diagnosis in unmanned aerial vehicles using LPV interval observers. *International Journal of Robust and Nonlinear Control* 2019; 29(16): 5456–5480.

8. Li S, Wang H, Aitouche A, Christov N. Unknown input observer design for faults estimation using linear parameter varying model. Application to wind turbine systems. In: IEEE. ; 2018: 45–50.

9. López-Estrada FR, Rotondo D, Valencia-Palomo G. A Review of Convex Approaches for Control, Observation and Safety of Linear Parameter Varying and Takagi-Sugeno Systems. *Processes* 2019; 7(11): 814.

10. López-Estrada FR, Santos-Estudillo O, Valencia-Palomo G, Gómez-Peñate S, Hernandez-Gutiérrez C. Robust qLPV Tracking Fault-Tolerant Control of a 3 DOF Mechanical Crane. *Mathematical and Computational Applications* 2020; 25(3): 48.

11. Bokor J, Balas G. Detection filter design for LPV systems – a geometric approach. *Automatica* 2004; 40(3): 511 - 518.

12. Ho LM. Robust Residual Generator Synthesis for Uncertain LPV Systems Applied to Lateral Vehicle Dynamics. *IEEE Transactions on Control Systems Technology* 2018; 27(3): 1275–1283.

13. Rodrigues M, Hamdi H, Theilliol D, Mechmeche C, BenHadj Braiek N. Actuator fault estimation based adaptive polytopic observer for a class of LPV descriptor systems. *International Journal of Robust and Nonlinear Control* 2015; 25(5): 673–688.

14. Bedioui N, Houimli R, Besbes M. Simultaneous sensor and actuator fault estimation for continuous-time polytopic LPV system. *International Journal of Systems Science* 2019; 50(6): 1290–1302.

15. Brizuela Mendoza J, Sorcia Vázquez FDJ, Guzmán Valdivia C, Osorio Sánchez R, Martínez García M. Observer design for sensor and actuator fault estimation applied to polynomial LPV systems: a riderless bicycle study case. *International Journal of Systems Science* 2018; 49(14): 2996–3006.

16. Li X, Zhu F. Simultaneous actuator and sensor fault estimation for descriptor LPV system based on $\mathcal{H}_\infty$ reduced-order observer. *Optimal Control Applications and Methods* 2016; 37(6): 1122–1138.

17. Li X, Zhu F. Simultaneous time-varying actuator and sensor fault reconstruction based on PI observer for LPV systems. *International journal of adaptive control and signal processing* 2015; 29(9): 1086–1098.

18. Rotondo D, López-Estrada FR, Nejjari F, Ponsart JC, Theilliol D, Puig V. Actuator multiplicative fault estimation in discrete-time LPV systems using switched observers. *Journal of the Franklin Institute* 2016; 353(13): 3176–3191.

19. Zhang H, Zhang G, Wang J. $\mathcal{H}_\infty$ Observer Design for LPV Systems with Uncertain Measurements on Scheduling Variables: Application to an Electric Ground Vehicle. *IEEE/ASME Transactions on Mechatronics* 2016; 21(3): 1659–1670.

20. Aouaouda S, Chadli M, Cocquempot V, Tarek Khadir M. Multi-objective H_-/H_∞ fault detection observer design for Takagi-Sugeno fuzzy systems with unmeasurable premise variables: descriptor approach. *International Journal of Adaptive Control and Signal Processing* 2013; 27(12): 1031–1047.

21. López-Estrada FR, Ponsart JC, Astorga-Zaragoza C, Theilliol D. Fault estimation observer design for descriptor-LPV systems with unmeasurable gain scheduling functions. In: IEEE. ; 2013: 269–274.

22. Hassanabadi AH, Shafiee M, Puig V. Actuator fault diagnosis of singular delayed LPV systems with inexact measured parameters via PI unknown input observer. *IET Control Theory & Applications* 2017; 11(12): 1894–1903.

23. Zhu K, Zhao J. Simultaneous fault detection and control for switched LPV systems with inexact parameters and its application. *International Journal of Systems Science* 2017; 48(14): 2909–2920.

24. Gómez-Peñate S, López-Estrada FR, Valencia-Palomo G, Rotondo D, Enríquez-Zárate J. Actuator and sensor fault estimation based on a proportional-integral quasi-LPV observer with inexact scheduling parameters. *IFAC-PapersOnLine* 2019; 52(28): 100–105.

25. Cai X, Liu Y, Zhang W. Control design for a class of nonlinear parameter varying systems. *International Journal of Systems Science* 2015; 46(9): 1638–1647.

26. Sala A, Ariño C, Robles R. Gain-Scheduled Control via Convex Nonlinear Parameter Varying Models. *IFAC-PapersOnLine* 2019; 52(28): 70–75.

27. Chen F, Kang S, Ji L, Zhang X. Stability and stabilisation for time-varying polytopic quadratic systems. *International Journal of Control* 2017; 90(2): 357–367.

28. Kanarachos S, Dizqah AM, Chrysakis G, Fitzpatrick ME. Optimal design of a quadratic parameter varying vehicle suspension system using contrast-based fruit fly optimisation. *Applied Soft Computing* 2018; 62: 463–477.

29. Rotondo D, Johansen TA. Analysis and design of quadratic parameter varying (QPV) control systems with polytopic attractive region. *Journal of the Franklin Institute* 2018; 355(8): 3488–3507.

30. Yang R, Rotondo D, Puig V. D-stable Controller Design for Lipschitz NLPV System. *IFAC-PapersOnLine* 2019; 52(28): 88–93.

31. Tan CP, Edwards C. An LMI approach for designing sliding mode observers. *International Journal of Control* 2001; 74(16): 1559–1568.

32. Utkin VI. *Sliding modes in control and optimization*. Springer Science & Business Media . 2013.

33. Edwards C, Spurgeon SK, Patton RJ. Sliding mode observers for fault detection and isolation. *Automatica* 2000; 36(4): 541–553.

34. Tan CP, Edwards C. Sliding mode observers for detection and reconstruction of sensor faults. *Automatica* 2002; 38(10): 1815–1821.

35. Brahim AB, Dhahri S, Hmida FB, Sellami A. An H_∞ sliding mode observer for Takagi–Sugeno nonlinear systems with simultaneous actuator and sensor faults. *International Journal of Applied Mathematics and Computer Science* 2015; 25(3): 547–559.

36. Chen L, Edwards C, Alwi H. Sensor fault estimation using LPV sliding mode observers with erroneous scheduling parameters. *Automatica* 2019; 101: 66–77.

37. Rotondo D, Sanchez HS, Nejjari F, Puig V. Analysis and design of linear parameter varying systems using LMIs. *Rev. Iberoam. Autom. Inform. Ind* 2019; 16: 1–14.

38. Youssef T, Chadli M, Karimi HR, Wang R. Actuator and sensor faults estimation based on proportional integral observer for TS fuzzy model. *Journal of the Franklin Institute* 2017; 354(6): 2524–2542.

39. Ichalal D, Marx B, Ragot J, Maquin D. State estimation of Takagi–Sugeno systems with unmeasurable premise variables. *IET Control Theory & Applications* 2010; 4(5): 897–908.

40. Elleuch I, Khedher A, Othman KB. Design of a proportional integral observer based on sliding mode principle for uncertain Takagi-Sugeno fuzzy systems: applications to a turbo-reactor. *International Journal of Automation and Control* 2018; 12(2): 179–194.

41. Adir VG, Stoica AM. Integral LQR control of a star-shaped octorotor. *Incas Bulletin* 2012; 4(2): 3.

42. Adir VG, Stoica AM, Whidborne JF. Sliding mode control of a 4Y octorotor. *UPB Sci. Bull., Series D* 2012; 74(4): 37–51.

43. Li T, Zhang Y, Gordon BW. Passive and active nonlinear fault-tolerant control of a quadrotor unmanned aerial vehicle based on the sliding mode control technique. *Proceedings of the Institution of Mechanical Engineers, Part I: Journal of Systems and Control Engineering* 2013; 227(1): 12–23.

44. Wang X, Sun S, Kampen vEJ, Chu Q. Quadrotor fault tolerant incremental sliding mode control driven by sliding mode disturbance observers. *Aerospace Science and Technology* 2019; 87: 417–430.

45. Saied M, Lussier B, Fantoni I, Shraim H, Francis C. Active versus passive fault-tolerant control of a redundant multirotor UAV. *The Aeronautical Journal* 2020; 124(1273): 385–408.

46. Bertrand S, Guénard N, Hamel T, Piet-Lahanier H, Eck L. A hierarchical controller for miniature VTOL UAVs: Design and stability analysis using singular perturbation theory. *Control Engineering Practice* 2011; 19(10): 1099–1108.

47. Ortiz-Torres G, Castillo P, Sorcia-Vázquez FD, et al. Fault estimation and fault tolerant control strategies applied to vtol aerial vehicles with soft and aggressive actuator faults. *IEEE Access* 2020; 8: 10649–10661.

48. Avram RC, Zhang X, Muse J. Quadrotor actuator fault diagnosis and accommodation using nonlinear adaptive estimators. *IEEE Transactions on Control Systems Technology* 2017; 25(6): 2219–2226.

49. Saied M, Lussier B, Fantoni I, Francis C, Shraim H, Sanahuja G. Fault diagnosis and fault-tolerant control strategy for rotor failure in an octorotor. In: IEEE. ; 2015: 5266–5271.

50. Alwi H, Edwards C. Sliding mode fault-tolerant control of an octorotor using linear parameter varying-based schemes. *IET Control Theory & Applications* 2015; 9(4): 618–636.

51. Tanaka K, Wang HO. *Fuzzy control systems design and analysis: a linear matrix inequality approach*. New York, USA: John Wiley & Sons . 2004.

52. Isermann R. Model-based fault-detection and diagnosis–status and applications. *Annual Reviews in control* 2005; 29(1): 71–85.

53. Saied M, Shraim H, Francis C, Fantoni I, Lussier B. Actuator fault diagnosis in an octorotor UAV using sliding modes technique: Theory and experimentation. In: IEEE. ; 2015: 1639–1644.

APPENDIX

$$\begin{aligned}\zeta_{1,1} &= \zeta_{1,2} = \zeta_{1,3} = \zeta_{1,4} = 12.72\\ \zeta_{2,1} &= \zeta_{2,2} = \zeta_{2,3} = \zeta_{2,4} = 2.27\\ \zeta_{3,1} &= \zeta_{3,2} = \zeta_{3,3} = \zeta_{3,4} = 6.70\end{aligned} \tag{79}$$

$$\mathcal{K}_1 = \begin{bmatrix}
-0.2211 & -0.2197 & -0.1291 & 2.1012 & -0.0306\\
-0.2241 & -0.2254 & -0.1401 & -0.0172 & 2.1136\\
-7.7174 & -7.7173 & 35.6925 & -0.5782 & -1.0323\\
-3.0836 & -3.0827 & -22.1310 & 37.0713 & -0.4230\\
-10.1879 & -10.1886 & 5.2328 & -0.7877 & 37.6282\\
-44.0791 & -44.0782 & 180.7771 & -3.4514 & -6.2712\\
23.9023 & -6.2429 & -2.7088 & 0.5251 & -0.8552\\
-6.2426 & 23.9030 & -2.7061 & -0.4711 & 0.1372\\
-6.3450 & -6.3449 & 30.0493 & -0.4701 & -0.8374\\
-6.5539 & -6.5535 & -4.0691 & 33.0435 & -0.9148\\
-6.6839 & -6.6838 & -4.4040 & -0.5110 & 33.4149\\
-0.8391 & -0.8384 & -1.6267 & 5.0231 & -0.1297\\
-1.0544 & -1.0553 & -2.1908 & -0.0867 & 6.2540\\
-8.2124 & -8.2122 & 31.9730 & -0.6713 & -1.2353\\
6.2580 & -1.6215 & -0.7695 & -0.1238 & -0.2229\\
-1.6214 & 6.2582 & -0.7688 & -0.1228 & -0.2249\\
-0.5912 & -0.5906 & -1.3828 & 3.6835 & -0.0923\\
-0.8218 & -0.8229 & -2.1400 & -0.0688 & 5.1672\\
-5.5539 & -5.5538 & 20.5901 & -0.4643 & -0.8539\\
8.5172 & -1.7943 & -2.8526 & -0.1465 & -0.2675\\
-1.7942 & 8.5174 & -2.8515 & -0.1450 & -0.2704
\end{bmatrix} \tag{80}$$

$$\mathcal{K}_2 = \begin{bmatrix}
-0.2210 & -0.2197 & -0.1294 & 2.1013 & -0.0306\\
-0.2243 & -0.2256 & -0.1397 & -0.0171 & 2.1135\\
-7.7214 & -7.7213 & 35.7032 & -0.5768 & -1.0343\\
-11.2530 & -11.2520 & 11.5652 & 36.4328 & -1.5917\\
-10.1857 & -10.1863 & 5.2302 & -0.7874 & 37.6272\\
-44.1030 & -44.1023 & 180.8426 & -3.4439 & -6.2832\\
23.8966 & -6.2486 & -2.6945 & 0.5251 & -0.8557\\
-6.2483 & 23.8973 & -2.6919 & -0.4711 & 0.1367\\
-6.3519 & -6.3518 & 30.0678 & -0.4696 & -0.8390\\
-6.5520 & -6.5516 & -4.0796 & 33.0453 & -0.9139\\
-6.6886 & -6.6885 & -4.3897 & -0.5104 & 33.4131\\
-0.8372 & -0.8365 & -1.6338 & 5.0235 & -0.1292\\
-1.0544 & -1.0553 & -2.1900 & -0.0867 & 6.2537\\
-8.2166 & -8.2164 & 31.9844 & -0.6699 & -1.2375\\
6.2574 & -1.6221 & -0.7682 & -0.1237 & -0.2230\\
-1.6220 & 6.2576 & -0.7675 & -0.1227 & -0.2250\\
-0.5900 & -0.5894 & -1.3872 & 3.6838 & -0.0920\\
-0.8218 & -0.8228 & -2.1394 & -0.0688 & 5.1670\\
-5.5567 & -5.5565 & 20.5976 & -0.4633 & -0.8554\\
8.5166 & -1.7949 & -2.8513 & -0.1465 & -0.2675\\
-1.7948 & 8.5168 & -2.8503 & -0.1450 & -0.2704
\end{bmatrix} \tag{81}$$

$$\mathcal{K}_3 = \begin{bmatrix} -0.2212 & -0.2199 & -0.1288 & 2.1012 & -0.0307 \\ -0.2243 & -0.2256 & -0.1395 & -0.0172 & 2.1135 \\ -7.7179 & -7.7178 & 35.6926 & -0.5770 & -1.0337 \\ -3.0937 & -3.0928 & -22.1069 & 37.0722 & -0.4262 \\ -4.7483 & -4.7490 & -17.2080 & -0.3615 & 38.4038 \\ -44.0812 & -44.0805 & 180.7754 & -3.4446 & -6.2792 \\ 23.9043 & -6.2409 & -2.7146 & 0.5254 & -0.8550 \\ -6.2406 & 23.9050 & -2.7119 & -0.4708 & 0.1374 \\ -6.3427 & -6.3426 & 30.0418 & -0.4692 & -0.8377 \\ -6.5554 & -6.5549 & -4.0683 & 33.0441 & -0.9153 \\ -6.6876 & -6.6876 & -4.3901 & -0.5111 & 33.4127 \\ -0.8397 & -0.8390 & -1.6259 & 5.0232 & -0.1298 \\ -1.0565 & -1.0574 & -2.1832 & -0.0870 & 6.2533 \\ -8.2129 & -8.2128 & 31.9730 & -0.6701 & -1.2368 \\ 6.2579 & -1.6216 & -0.7693 & -0.1237 & -0.2230 \\ -1.6215 & 6.2581 & -0.7686 & -0.1228 & -0.2250 \\ -0.5916 & -0.5910 & -1.3822 & 3.6836 & -0.0924 \\ -0.8233 & -0.8244 & -2.1345 & -0.0691 & 5.1666 \\ -5.5543 & -5.5542 & 20.5902 & -0.4634 & -0.8549 \\ 8.5173 & -1.7943 & -2.8526 & -0.1465 & -0.2675 \\ -1.7942 & 8.5175 & -2.8516 & -0.1450 & -0.2704 \end{bmatrix} \tag{82}$$

$$\mathcal{K}_4 = \begin{bmatrix} -0.2209 & -0.2196 & -0.1298 & 2.1014 & -0.0307 \\ -0.2242 & -0.2255 & -0.1397 & -0.0171 & 2.1134 \\ -7.7171 & -7.7170 & 35.6919 & -0.5755 & -1.0353 \\ -11.2563 & -11.2553 & 11.5672 & 36.4340 & -1.5918 \\ -4.7400 & -4.7408 & -17.2270 & -0.3585 & 38.4021 \\ -44.0771 & -44.0766 & 180.7733 & -3.4359 & -6.2885 \\ 23.9016 & -6.2436 & -2.7067 & 0.5254 & -0.8558 \\ -6.2433 & 23.9023 & -2.7041 & -0.4708 & 0.1366 \\ -6.3455 & -6.3455 & 30.0512 & -0.4687 & -0.8393 \\ -6.5486 & -6.5482 & -4.0908 & 33.0468 & -0.9142 \\ -6.6879 & -6.6879 & -4.3864 & -0.5103 & 33.4112 \\ -0.8373 & -0.8367 & -1.6346 & 5.0238 & -0.1292 \\ -1.0560 & -1.0569 & -2.1837 & -0.0869 & 6.2531 \\ -8.2120 & -8.2119 & 31.9722 & -0.6684 & -1.2385 \\ 6.2580 & -1.6215 & -0.7696 & -0.1236 & -0.2232 \\ -1.6214 & 6.2582 & -0.7689 & -0.1226 & -0.2251 \\ -0.5901 & -0.5895 & -1.3878 & 3.6840 & -0.0919 \\ -0.8229 & -0.8240 & -2.1350 & -0.0690 & 5.1665 \\ -5.5536 & -5.5536 & 20.5896 & -0.4623 & -0.8561 \\ 8.5172 & -1.7943 & -2.8526 & -0.1464 & -0.2676 \\ -1.7942 & 8.5174 & -2.8516 & -0.1450 & -0.2705 \end{bmatrix} \tag{83}$$

AUTHOR BIOGRAPHY

Samuel Gómez-Peñate is a Ph.D. student at the Department of Electronic Engineering at Tecnológico Nacional de México/Instituto Tecnológico de Tuxtla Gutiérrez. He received his M.Sc. degree in Electronic Engineering in 2016 from the National Center of Research and Technological Development (CENIDET), Mexico. His research interests are centered on fault diagnosis, fault-tolerant control systems, Takagi-Sugeno systems, LPV systems, and its applications.

Francisco-Ronay López-Estrada received his Ph.D. in Automatic Control from the University of Lorraine, France, in 2014. He has been with "Tecnológico Nacional de México/IT Tuxtla Gutiérrez", Mexico, as a lecturer since 2008. He received his M.Sc. degree in Electronic Engineering in 2008 from the National Center of Research and Technological Development (CENIDET), Mexico. He has led several funded research projects, Ph.D. and Master thesis. His research interests are descriptor systems, TS systems, fault detection, fault-tolerant control, and their applications to robotics and pipeline leak detection systems.

Guillermo Valencia-Palmo was born in Merida, Yucatan, Mexico, in 1980. He received an Engineering degree in Electronics from the Instituto Tecnológico de Mérida, Mexico, in 2003; an M.Sc. in Automatic Control from the National Center of Research and Technological Development (CENIDET), Mexico, in 2006; and a Ph.D. degree in Automatic Control and Systems Engineering from The University of Sheffield, U.K., in 2010. Since 2010, Dr. Guillermo Valencia-Palomo has been a full-time professor at Tecnológico Nacional de México/I.T. Hermosillo, Mexico. His research interests include predictive control, descriptor systems, linear parameter varying systems, fault detection, fault tolerant control systems, and their applications to different physical systems.

Damiano Rotondo was born in Francavilla Fontana, Italy, in 1987. He received the B.Sc. degree in Computer Engineering from the Second University of Naples, Italy, the M.Sc. degree in Automation Engineering from the University of Pisa, Italy, and the Ph.D. degree in Automatic Control, Robotics and Computer Vision from the Universitat Politècnica de Catalunya, Spain in 2008, 2011 and 2016, respectively. Since February 2020, he is an Associate Professor at the Department of Electrical Engineering and Computer Science (IDE) of the University of Stavanger (UiS), Norway. His main research interests include gain-scheduled control systems, fault detection and isolation (FDI) and fault tolerant control (FTC) of dynamical systems.

María-Eusebia Guerrero-Sánchez received the Ph.D. degree in Electronic Engineering from the National Center for Research and Technological Development, Mexico, in 2017. She has held post-doctoral positions at the French-Mexican Laboratory on Computer Science and Control UMI-LAFMIA 3175 at CINVESTAV, Mexico. She is currently full-time professor at Tecnológico Nacional de México/I.T. Hermosillo, Mexico, and member of the National Research System SNI since 2017. Her research interests are focused on passivity-based control, nonlinear control, and UAVs.